Synthesis and Characterization of Copper Complexes Containing the Tripodal N_7 Ligand Tris{2-[(pyridin-2-ylmethyl)amino]ethyl}amine (= *N′*-(Pyridin-2-ylmethyl)-*N,N*-bis{2-[(pyridin-2-ylmethyl)amino]ethyl}ethane-1,2-diamine): Equilibrium, Spectroscopic Data, and Crystal Structures of Mono- and Trinuclear Copper(II) Complexes

by **Christian Gérard**[a]), **Aminou Mohamadou***[a]), **Jérôme Marrot**[b]), **Stéphane Brandes**[c]), and **Alain Tabard**[c])

[a]) GRECI, Groupe de Recherche en Chimie Inorganique, Faculté des Sciences, Université de Reims Champagne-Ardenne, Moulin de la Housse, BP 1039, F-51687 Reims Cedex 2 (e-mail: aminou.mohamadou@univ-reims.fr)

[b]) Université de Versailles Saint-Quentin-en-Yvelines, Institut Lavoisier, IREM, UMR CNRS C 8637, 45 Avenue des Etats-Unis, F-78035 Versailles

[c]) LIMSAG, Laboratoire d'Ingénierie Moléculaire pour la Séparation et les Applications des Gaz, UMR CNRS 5633, Faculté des Sciences 'Gabriel', Université de Bourgogne, 6 Boulevard Gabriel, F-21100 Dijon

The stability constants of the Cu^{II} chelates with the tripodal heptadentate ligand tris{2-[(2-pyridylmethyl)amino]ethyl}amine (= *N′*-(pyridin-2-ylmethyl)-*N,N*-bis{2-[(pyridin-2-ylmethyl)amino]ethyl}ethane-1,2-diamine; tpaa), determined by potentiometry and UV spectrometry, show the formation of $[Cu(tpaaH)]^{3+}$ and $[Cu(tpaa)]^{2+}$ species. In the solid state, two mononuclear Cu^{II} compounds, $[Cu(tpaa)](PF_6)_2$ (**1**) and $[Cu(tpaaH)](ClO_4)_3 \cdot H_2O$ (**2**), and one trinuclear $[Cu_3(tpaa)_2(ClO_4)_2](ClO_4)_4 \cdot 2\,H_2O$ (**3**) complex were isolated and characterized by IR, UV/VIS, and EPR spectroscopy. An X-ray structure of the mononuclear protonated complex **2** shows that the Cu^{2+} ion has a distorted square-pyramidal geometry ($\tau = 0.21$). and the proton is bound to the secondary-amine function of one uncoordinated arm of the tripod ligand (*Fig. 4*). The crystal lattice for **2** is stabilized by the H-bonds between the N-atom of the free pyridinyl group with the proton of the free secondary-amine function of the neighboring molecule. The linear trinuclear complex **3** consists of two entities of the pyramidal mononuclear complex **1** bound to the third central Cu^{2+} ion by the free unprotonated arms of the ligands in equatorial position (*Fig. 5*). The octahedral geometry of the third Cu^{II} atom is achieved by two perchlorate anions in the axial positions. The redox properties of **1**–**3** compounds was examined by cyclic voltammetry.

1. Introduction. – Much current interest in the biomimetic chemistry of Cu^{II} complexes with polydentate ligands carrying donor N-atoms has been stimulated by the crystal-structure determination of several enzymes like ascorbate oxidase and its derivatives [1], and ceruloplasmin [2]. These proteins belong to the group of multicopper oxidase and contain dinuclear or trinuclear metal clusters in which Cu-atoms are bound to N-atoms of histidine residues. The Cu-ion in these metalloenzymes plays the role of catalyst to overcome the unfavorable kinetics of reactions of organic substances with O_2 in biological systems. For a better understanding of the mechanisms of these reactions in abiotic systems as well as the utility of this kind of compound as catalysts for selective reactions in the chemical industry, Cu^{II} complexes with various chelating ligands that reproduce structural or functional features of enzymes centers have been reported [3].

We previously reported the coordination of Ni- [4], and Cu- and Zn-atoms [5] with linear hexadendate ligands involving two pyridinylmethyl groups and containing donor N- and O-atoms or N- and S-atoms. These studies show that the thermodynamic stability, the structural configuration, and the redox properties of these mononuclear complexes depend on the nature of the two central donor heteroatoms. In our most recent approach, we have described the mono- and dinuclear Zn^{II} complexes [6] with a heptadentate tripod ligand tris{2-[(pyridin-2-ylmethyl)amino]ethyl}amine (= *N′*-(pyridin-2-ylmethyl)-*N,N*-bis{2-[(pyridin-2-ylmethyl)amino]ethyl}ethane-1,2-diamine; tpaa). The Fe^{III} [7], Fe^{II} [8], and Mn^{II} [9] complexes with tpaa were also previously reported as models of superoxide dismutase (SOD). *Morgenstern* and co-workers [8][9] characterized the structures of $[Mn(tpaa)]^{2+}$ and $[Fe(tpaa)]^{2+}$ compounds with a coordination number of seven, achieved by only one ligand. *Callhan* and co-workers [10] reported the dinuclear compound obtained with Ni^{2+} ion and tpaa.

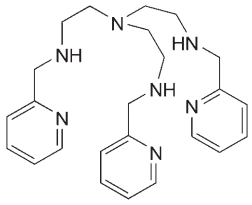

tpaa

In this paper, we report the syntheses of two mononuclear and one trinuclear Cu^{II} complexes, $[Cu(tpaa)](PF_6)_2$ (**1**), $[Cu(tpaaH)](ClO_4)_3 \cdot H_2O$ (**2**), and $[Cu_3(tpaa)_2(ClO_4)_2](ClO_4)_4 \cdot 2\,H_2O$ (**3**) as well as the equilibrium constants of the metal chelates formed by tpaa in the aqueous solution. The complete spectroscopic data, X-ray crystal-structure determinations, and electrochemical studies are also reported.

2. Results and Discussion. – 2.1. *Major Species in Aqueous Solution*. Protometric titrations with 0.1M KOH were carried out for a large range of ratios C_L/C_{Cu} varying from 1.0 to 9.8. *Fig. 1* shows the curves $\bar{h}$ *vs.* pH for tpaa alone ($1.25 \cdot 10^{-3}$ M), and for $C_L = C_{Cu} = 1.29 \cdot 10^{-3}$ M; $\bar{h}$ is the mean number of bound protons per mol of ligand: given by *Eqn. 1*, where n is the number of protons of the neutral species of the ligand, C_B the initial concentration of strong base, and C_H the initial concentration of strong acid. The ligand alone was studied in detail earlier [6]: the logarithms of the successive protonation constants $\log K_h$ (equilibrium $\left(LH_{(h-1)}\right)^{(h-1)^+} + H^+ \rightleftharpoons (LH_h)^{h+}$) are $\log K_1 = 9.12(0.01)$, $\log K_2 = 8.14(0.01)$, $\log K_3 = 6.91(0.01)$, $\log K_4 = 2.50(0.01)$, and $\log K_5 = 1.0(0.3)$. The presence of Cu^{2+} leads to a dramatic decrease of $\bar{h}$ values from pH *ca.* 2.5 on; a plateau at $\bar{h} = 1$ corresponds to the quantitative formation of the $[Cu(tpaaH)]^{3+}$ species, and its deprotonation into $[Cu(tpaa)]^{2+}$ appears in the pH range 5–8; above pH 8, $\bar{h}$ values decrease slightly below zero, which seems to indicate the formation of hydroxo species (this phenomenon does not appear for the ratio $C_L/C_{Cu} > 1$).

$$\bar{h} = \frac{1}{C_L}(nC_L - [H^+] + [OH^-] - C_B + C_H) \quad (1)$$

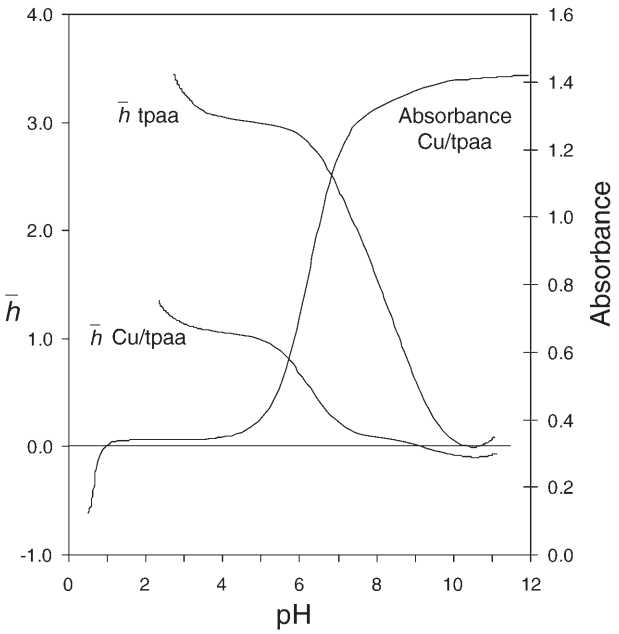

Fig. 1. *Average number* $\bar{h}$ *of bound protons per mol of ligand for tpaa alone* ($1.25 \cdot 10^{-3}$ M) *and in the presence for* Cu^{2+} ($C_L = C_{Cu} = 1.29 \cdot 10^{-3}$ M). The concentrations for the superimposed absorbance curve at 730 nm are $C_L = C_{Cu} = 8.30 \cdot 10^{-3}$ M.

Spectrophotometric titrations were carried out for $C_L = C_{Cu} = 8.30 \cdot 10^{-3}$ M with 0.1M KOH and 1M HNO_3; the absorbance *vs.* pH plot (see *Fig. 1*) is in agreement with the pH ranges of the major species. It presents a large plateau in the pH range *ca.* 1–5 corresponding to $[Cu(tpaaH)]^{3+}$; no true plateau appears for $pH > 8$, which is consistent with the probable formation of hydroxo species.

2.2. *Equilibrium Constants.* The equilibrium constants are usually determined from protometric titrations with the help of refinement programs, according to the general equilibrium of *Eqn. 2*[1]). This was possible for the constant β_{110} of the complex $[Cu(tpaa)]^{3+}$ (noted CuL^1)) which was determined from protometric titrations as well as from a spectrophotometric titration. Unfortunately, the equilibrium between Cu^{2+} and $[Cu(tpaaH)]^{2+}$ (denoted $CuLH^1$)), occurs only in a very acidic pH range. Thus, protometric titrations are useless because the equilibrium does not influence the pH values. Only an estimate was made from the spectrophotometric titration ($C_{Cu} = C_L = 8.30 \cdot 10^{-3}$ M; $pH < 0.5$) by means of *Eqn. 3*.

$$Cu^{2+} + lL + hH^+ \rightleftharpoons Cu_mL_lH_h \quad \beta_{mlh} = \frac{[Cu_mL_lH_h]}{[Cu^{2+}]^m[L]^l[H^+]^h} \tag{2}$$

[1]) For convenience, brackets enclosing formulae of complexes and most charges are omitted in *Eqn. 2* and the following.

$$Cu^{2+} + LH_5 \rightleftharpoons CuLH + 4\ H^+ \quad K_{111} = \frac{[CuLH][H^+]^4}{[Cu^{2+}][LH_5]} \tag{3}$$

The significant forms of the ligand in this pH range are LH_5, LH_4, and CuLH; the only absorbing species are Cu^{2+} and CuLH (see *Eqn. 4*; ε = average molar extinction coefficient). ε_{Cu} is obtained from direct measurements, and ε_{CuLH} is calculated from the equilibrium between CuLH and CuL by means of a least-squares method (see below). For the pH value such as $[Cu^{2+}] = [CuLH] = 1/2\ C_{Cu}$, ε is given by *Eqn. 5*.

$$\varepsilon\ C_{Cu} = \varepsilon_{Cu}\ [Cu^{2+}] + \varepsilon_{CuLH}\ [CuLH] \tag{4}$$

$$\varepsilon = \frac{1}{2}(\varepsilon_{Cu} + \varepsilon_{CuLH}) \tag{5}$$

$[LH_5]$ is easily obtained from *Eqn. 6*. From measurements at 610 nm, the value obtained for pH 0.67 is $K_{111} = 1.0$ ($\log \beta_{111} = 27.7$).

$$C_L = [CuLH] + [LH_5] + [LH_4] = \frac{1}{2}C_{Cu} + [LH_5]\left(1 + \frac{K_{a1}}{[H^+]}\right) \tag{6}$$

For the equilibrium of *Eqn. 7*, K_{110} and α are defined as shown. The average molar extinction coefficient ε is a function of α (*Eqn. 8*):

$$CuLH \rightleftharpoons CuL + H^+ \qquad K_{110} = K_a = \frac{[CuL][H^+]}{[CuLH]} = \frac{\alpha[H^+]}{(1-\alpha)} \qquad \alpha = \frac{K_{110}}{K_{110} + [H^+]} \tag{7}$$

$$\varepsilon = \varepsilon_{CuHL} + (\varepsilon_{CuL} - \varepsilon_{CuHL})\ \alpha \tag{8}$$

The best value of K_{110} leads to the best 'straight line' for $\varepsilon = f(\alpha)$. The value so obtained at 730 nm is $\log K_{110} = -6.26$ ($\log \beta_{110} = 21.4$). These above constants depend on $\log \beta_{111}$ obtained from spectrophotometric measurements and so their standard deviations could not be determined. Protometric titrations were refined with the help of the program PROTAF [11]; the value $\log \beta_{111} = 27.7$ obtained by the spectrophotometric titration was introduced in the calculation process but not refined. The value obtained from five different protometric titrations is $\log \beta_{110} = 21.5$. *Fig. 2* represents the distribution curves obtained with the help of HySS [12] for equimolar solutions (10^{-3} M).

2.3. *Complex Structures in Aqueous Solution.* The least-squares method, in which an equilibrium between only two absorbing species is assumed, was used to obtain the VIS spectra of $[Cu(tpaaH)]^{3+}$ and $[Cu(tpaa)]^{2+}$ in the pH range 5–8. The spectrum of $[Cu(tpaaH)]^{3+}$ ($\tilde{\nu}_{max}$ 16450 cm^{-1}; $\varepsilon = 150$ M cm^{-1}; see *Fig. 3*) is similar to those described in [13] for analogous CuN_5 chromophores, which are in agreement with a square-pyramidal geometry. The electronic spectrum of the $[Cu(tpaa)]^{2+}$ species presents a strong band ($\tilde{\nu}_{max}$ 15600 cm^{-1}; $\varepsilon = 174$ M cm^{-1}; see *Fig. 3*) with a lower-energy shoulder (13500 cm^{-1}) indicating probably the continuous variation of the coordination sphere around the Cu^{2+} ion, in agreement with the plasticity of Cu^{II} complexes [14].

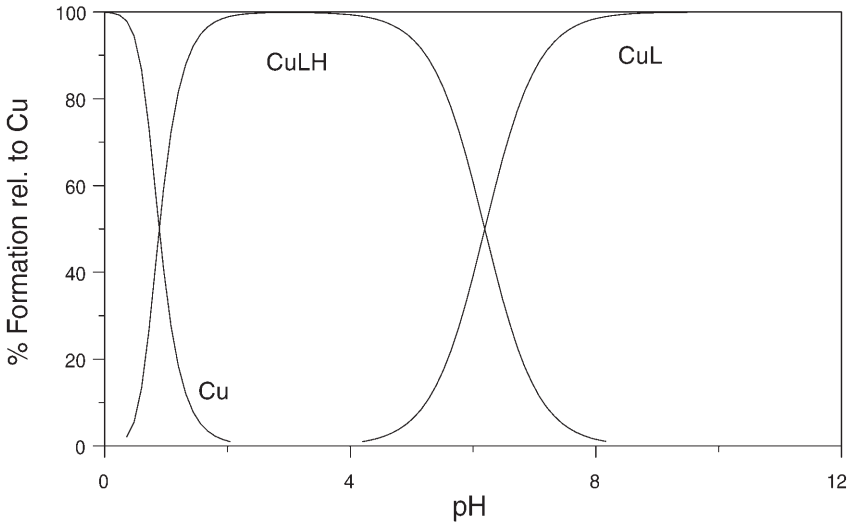

Fig. 2. *Distribution curves of Cu^{II}/tpaa complexes*[1]). $C_L = C_{Cu} = 10^{-3}$ M.

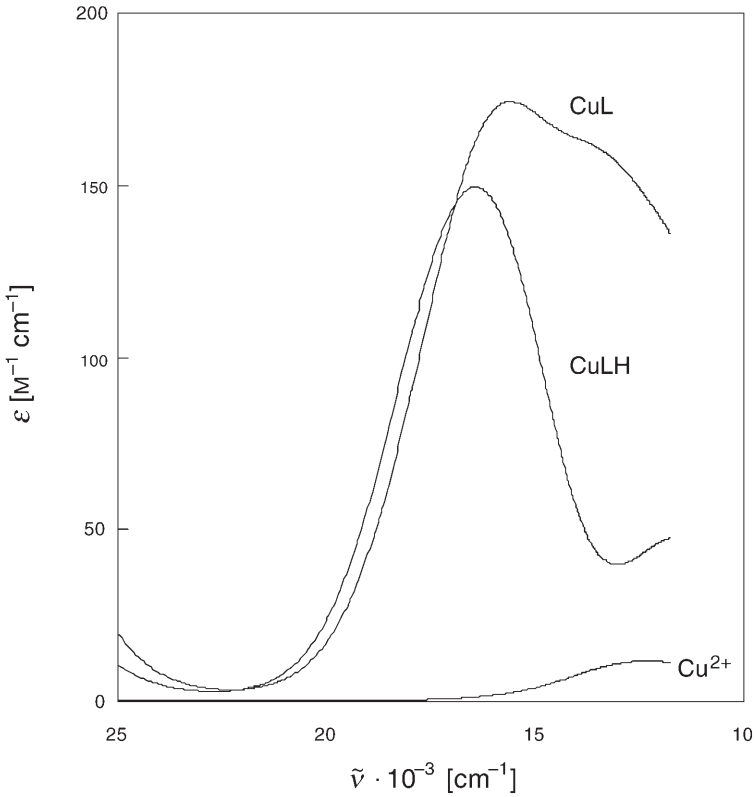

Fig. 3. *Spectra of Cu^{II}/tpaa complexes calculated from the spectrophotometric titrations*[1])

2.4. *X-Ray-Diffraction Studies.* The crystal structures of the complexes [Cu(tpaaH)]$(ClO_4)_3 \cdot H_2O$ (**2**) and $[Cu_3(tpaa)_2(ClO_4)_2](ClO_4)_4 \cdot 2\,H_2O$ (**3**) were determined by single-crystal X-ray-diffraction analysis (*Table 1*).

Table 1. *Crystal Data and Structure-Refinement Parameters for Compounds* **2** *and* **3**

	2	**3**
Formula	$C_{24}H_{36}Cl_3N_7O_{13}Cu$	$C_{48}H_{70}Cl_6N_{14}O_{26}Cu_3$
M_r	800.49	1662.50
Crystal system	monoclinic	monoclinic
Space group	$P2_{1/n}$	$P2_{1/n}$
a [Å]	11.9759(2)	12.1299(2)
b [Å]	17.5978(1)	17.5222(3)
c [Å]	15.6140(2)	15.5217(1)
α [°]	90	90
β [°]	101.435(1)	100.041(1)
γ [°]	90	90
U [Å^3]	3225.32(7)	3248.49(8)
T [K]	293(2)	296(2)
Z	4	2
$\mu(\mathrm{Mo}K_\alpha)$ [mm^{-1}]	1.001	1.313
$F000$	1652	1706
Reflections measured	17092	22333
Unique reflections collected	5670	8387
Goodness-of-fit on F^2	1.060	1.038
$wR(F^2)$	0.1565	0.1596
$R_1(I > 2\sigma(I))$	0.0593	0.0580
R_{int}	0.0382	0.0293

[Cu(tpaaH)](ClO$_4$)$_3 \cdot$ H$_2$O (**2**). The crystal-structure determination reveals that crystals of **2** consist of $[Cu(tpaaH)]^{3+}$ cations well separated from ordered perchlorate anions. The Cl–O bond lengths and the O–Cl–O angles are consistent with those reported earlier [15]. A view of the cation with the labeling scheme is shown in F*ig. 4,a*. Principal bond distances and angles are listed in *Table 2*.

Although the protonated ligand tpaaH$^+$ is potentially hexadentate, the Cu^{II} complex has a distorted square-pyramidal geometry. Four N-atoms from two pyridinyl groups (N(1) and N(31)), from one secondary-amine function (N(8)), and from the tertiary-amine function (N(11)) form the base of a square pyramid, and the donor N-atom of one of the three secondary-amine functions (N(24)) occupies the apical position. Thus, one of the three (pyridinylmethyl)amino groups remains uncoordinated, with a proton bound to its amino N-atom (= N(amino)). The Cu–N(py) bond length (average, 1.996 Å) is comparable to those observed in other five-coordinate complexes where the Cu^{2+} ion is bound to a pyridinyl group [16]. The longest apical bond Cu–N(amino) (Cu–N(24) = 2.202(4) Å) reflects a weak axial interaction as expected for *Jahn–Teller*-sensitive Cu^{II} complexes. The angle between the *trans*-positioned basal N-atoms (N(8)–Cu–N(31) = 174.40(17)°), although less than the expected 180°, is in the range for *SP* Cu^{II} complexes (160–170°) in which the Cu^{II} center lies slightly above the basal plane [17]. So the geometry around the Cu^{2+} ion is best described as distorted square-pyramidal with the structural index $\tau = 0.21$ ($\tau = (\beta - \alpha)/60$, where β = N(8)–Cu–N(31) = 174.4(2)° and α = N(1)–Cu–N(11) =

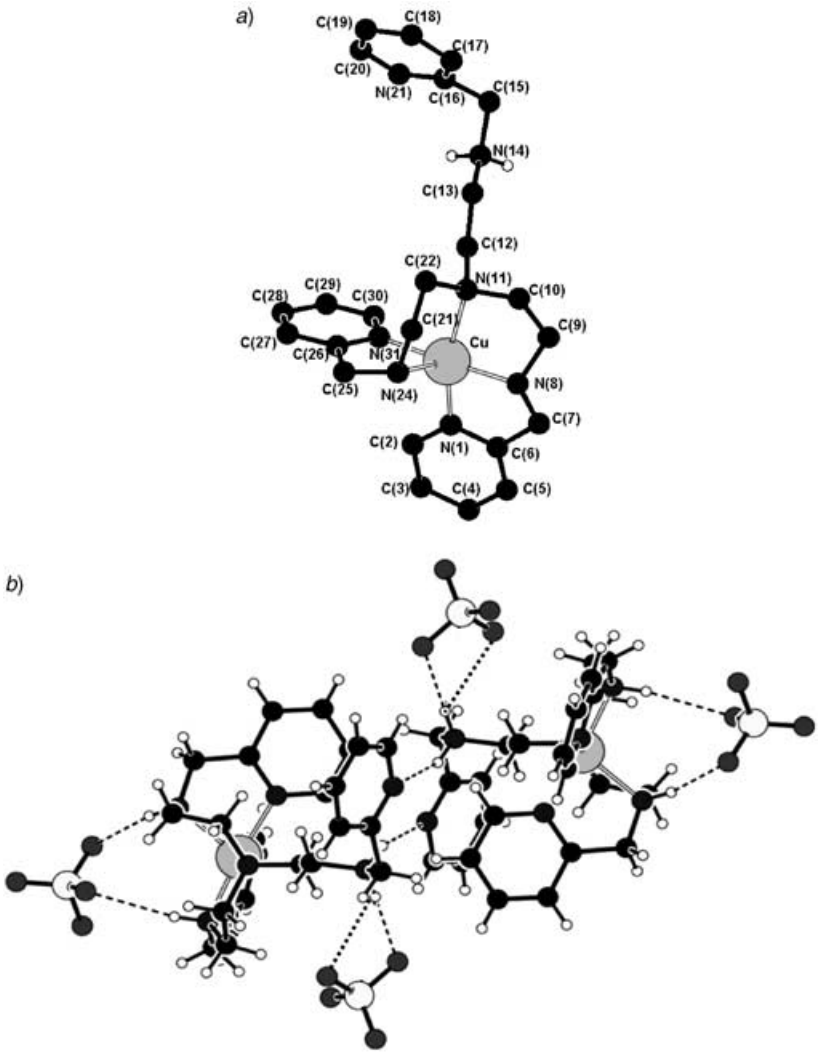

Fig. 4. a) *PLUTON Projection of the complex cation [Cu(tpaaH)]*$^{3+}$ *of* **2** (other H-atoms and the uncoordinating perchlorate anions are omitted for clarity). b) *H-Bonds in compound* **2**. Arbitrary atom numbering.

161.8(2)°); for perfect square-pyramidal and trigonal-bipyramidal geometries, the value of τ is zero and unity, respectively [18].

In the crystal lattice of compound **2**, two complex units interact (*Fig. 4*,*b*) *via* N(py)$\cdots$HN(amino) H-bonds of their uncoordinated arm, the distance N(py)$\cdots$HN being 2.897 Å. The other H-bonds are *via* of the type O$\cdots$HN between the O-atoms of four perchlorate anions and the HN of the six secondary-amine functions belonging to the two complex units (O(1)$\cdots$HN(24) = 3.123 Å, O(3)$\cdots$HN(8) = 3.406 Å, O(6)$\cdots$HN(14) = 2.865 Å) (see *Fig. 4*,*b*).

Table 2. *Selected Bond Lengths and Angles for Complexes* **2** *and* **3**. Arbitrary numbering.

Bond lengths [Å]		Bond angles [°]			
[Cu(tpaah)](ClO$_4$)$_3$·H$_2$O (**2**)					
Cu–N(1)	1.994(3)	N(1)–Cu–N(8)	83.13(15)	N(8)–Cu–N(24)	104.73(18)
Cu–N(8)	1.990(4)	N(1)–Cu–N(11)	161.80(14)	N(8)–Cu–N(31)	174.40(17)
Cu–N(11)	2.141(4)	N(1)–Cu–N(24)	112.57(16)	N(11)–Cu–N(24)	83.76(17)
Cu–N(24)	2.202(4)	N(1)–Cu–N(31)	95.31(15)	N(11)–Cu–N(31)	95.24(14)
Cu–N(31)	1.996(4)	N(8)–Cu–N(11)	84.95(14)	N(24)–Cu–N(31)	80.85(18)
[Cu$_3$(tpaa)$_2$](ClO$_4$)$_6$·2 H$_2$O (**3**)					
Cu(1)–N(1)	2.019(3)	N(1)–Cu(1)–N(8)	82.95(13)	N(11)–Cu(1)–N(21)	81.88(15)
Cu(1)–N(8)	1.996(3)	N(1)–Cu(1)–N(11)	162.98(12)	N(14)–Cu(1)–N(21)	95.24(14)
Cu(1)–N(11)	2.150(3)	N(1)–Cu(1)–N(14)	110.51(15)	N(24)–Cu(2)–N(25)	82.65(11)
Cu(1)–N(14)	2.205(4)	N(1)–Cu(1)–N(21)	95.39(13)	N(24)–Cu(2)–N(25A)	97.34(11)
Cu(1)–N(21)	1.996(3)	N(8)–Cu(1)–N(11)	84.61(13)	N(25)–Cu(2)–N(25A)	180.00(10)
Cu(2)–N(24)	2.058(3)	N(8)–Cu(1)–N(14)	104.12(19)	N(24)–Cu(2)–N(24A)	180.00(10)
Cu(2)–N(25)	2.000(3)	N(8)–Cu(1)–N(21)	173.98(17)	N(24)–Cu(2)–O(1)	84.80(2)
Cu(2)–O(1)	2.782(3)	N(11)–Cu(1)–N(14)	83.78(15)	N(25)–Cu(2)–O(1)	85.25(2)

[Cu$_3$(tpaa)$_2$(ClO$_4$)$_2$](ClO$_4$)$_4$·2 H$_2$O (**3**). The crystals of **3** consist of trinuclear (Cu(1), Cu(2), and Cu(1A)) cations, perchlorate anions, and H_2O molecules of crystallization. A PLUTON drawing is shown in *Fig. 5*, and important bond lengths and angles are listed in *Table 2*. The complex cation is arranged around a symmetry center, located at the central Cu^{2+} ion Cu(2), which is octahedrally coordinated with four N-

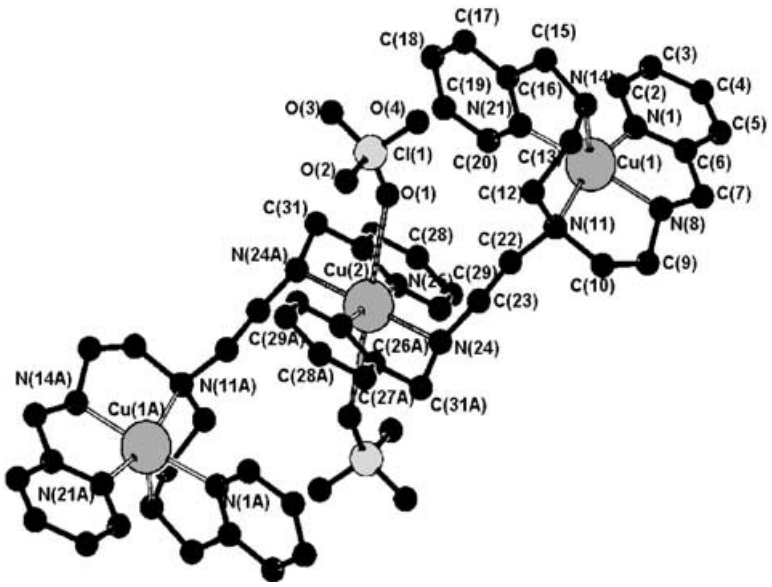

Fig. 5. *PLUTON Projection of the complex cation [Cu$_3$(tpaa)$_2$(ClO$_4$)$_2$]$^{4+}$ of* **3**. H-Atoms and the uncoordinating perchlorate anions are omitted for clarity. Atoms marked with 'A' are generated by an inversion center. Arbitrary atom numbering.

atoms from two (pyridinylmethyl)amino groups of the two free arms of two tpaa ligands in the equatorial plane; the pyridinyl N-atoms (N(25) and N(25A)) and the secondary-amine N-atoms (N(24) and N(24A)) are each mutually *trans*-positioned. The hexacoordination of Cu(2) is achieved by two O-atoms (O(1) and O(1A)) of two perchlorate anions in the axial positions; the letter A indicates the atoms generated by the center of symmetry. The equatorial bond distances Cu(2)–N(py) (2.000(3) Å) and Cu(2)–N(amino) (2.058(3) Å) are slightly different, whereas those of the axial Cu(2)–O(perchlorate) (2.782(2) Å), which are much longer, reflect a weak axial interaction, as expected for *Jahn–Teller*-sensitive Cu^{II}. The bond angles N(24)–Cu(2)–N(24A), N(25)–Cu(2)–N(25A), and O(1)–Cu(2)–O(1A) are all equal to 180.00(2)°, where N(24)–Cu(2)–O(1) and N(25)–Cu(2)–O(1) are 84.80° and 85.25°, respectively, indicating that the Cu(2) atom has an O_h symmetry. The central Cu(2) atom is connected to both Cu(1) and Cu(1A) atoms *via* (pyridinylmethyl)amino groups (one arm of each tpaa ligand), leading to quite long Cu–Cu separations (Cu(1)–Cu(2), 6.296 Å; Cu(1)–Cu(1A), 12.593 Å). Each of the terminal (Cu(1) and Cu(1A)) atoms has the distorted square-pyramidal geometry ($\tau = 0.18$) of the cation of compound **2** described above.

Each trinuclear subunit forms a trimeric unit *via* H-bonds between one O-atom of each of the two *trans*-positioned ClO_4^- ligands and one of the secondary-amine functions of the tpaa ligand of the neighboring trinuclear complex cation (O···HN = 3.141 Å). This H-bonding system forms an interesting two-dimensional sheet-like array. The uncoordinated perchlorate anions and H_2O molecules of crystallization stabilize the crystal lattice by other H-bonds involving their O-atoms and the remaining secondary-amine functions of the ligands, thus creating a polymeric structure.

We can note that the crystal structures of **2** and **3** appear to be almost identical. The difference is that the position occupied by Cu(2) in compound **3** is replaced in the crystal lattice of **2** by two protons.

2.5. *Spectroscopic Studies. IR Spectra*. IR Spectra of complexes **1**–**3** are similar in pattern to the one of the ligand tpaa. For all the three compounds, small shifts are observed for the characteristic secondary-amine bands (*ca.* 3400–3060 cm^{-1}) and those of the pyridinyl rings (*ca.* 1620–1610 cm^{-1}) to lower and higher energies, respectively. These vibrations are similar to those found in the analogous series of Cu^{II} complexes with ligands containing pyridinyl groups and five-membered chelate rings [19]. The absence of the in-plane vibration at *ca.* 610 cm^{-1} for complexes **1** and **3** is consistent with the complexation of all the pyridinyl groups [20] with Cu^{2+} ion. PF_6^- Anions in complex **1** and ClO_4^- Anions in compounds **2** and **3** are characterized by broad and strong bands at *ca.* 845 and 1090 cm^{-1}, respectively.

Absorption Spectra. The electronic spectra of **1**–**3** in the solid state are not different from those obtained in MeCN solution. The absorption spectra of these complexes exhibit essentially similar patterns in the 250–400 nm region, with two strong bands possibly due to intraligand [21] and charge-transfer transitions. In the VIS region, complex **1** displays a single large and unsymmetric band at 680 nm with a low value of the molar extinction coefficient ($\varepsilon = 70$ M^{-1} cm^{-1}). This spectrum closely resembles those of other six-coordinate CuN_6 chromophores [19][20] and suggests a tetragonal-distorted octahedral geometry around the Cu^{2+} ion [22]. It must be noted that the spectrum of complex **1** in MeCN solution is completely different from the one obtained

in the equilibrium studies for the $[Cu(tpaa)]^{2+}$ species in aqueous solution, which is probably due to solvent-induced structural changes in aqueous solution. Complexes **2** and **3** exhibit very similar VIS spectra (in the solid state and in MeCN solution) with a single symmetrical band at 668 nm ($\varepsilon = 148$ M^{-1} cm^{-1}) and 615 nm ($\varepsilon = 323$ M^{-1} cm^{-1}), respectively, in agreement with their crystal structure. This feature is characteristic of a square-based pyramidal geometry around the Cu^{2+} ion [23]. It is important to note that the trinuclear compound **3** does not present any d-d transition corresponding to the central Cu^{2+} ion, neither in the solid state nor in MeCN solution.

EPR Studies. The X-band EPR spectra of complexes **1**–**3** were recorded in fluid or frozen DMF/toluene at 293 and 100 K, respectively (*Fig. 6*), or in the polycrystalline state at 100 K. The isotropic and anisotropic hyperfine coupling constants A and g values are summarized in *Table 3*. The anisotropic spectra exhibit both parallel and perpendicular contributions for Cu^{II}, the transition associated to the parallel spectrum being split into four lines corresponding to the hyperfine coupling of the unpaired electron with the nuclear spin of the Cu^{2+} ion. Because the low-field parallel lines are rather broad, they show no evidence of ligand ^{14}N ($I = 1$) superhyperfine couplings. The EPR spectra showing anisotropic magnetic symmetry are typical of a nearly axially

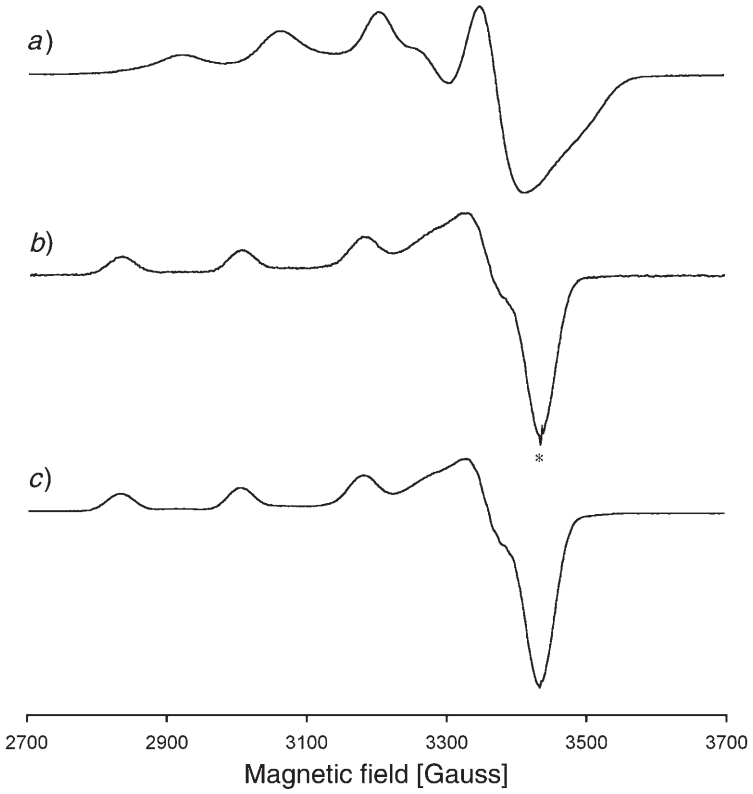

Fig. 6. *EPR Spectra at 100 K of* a) **1**, b) **2**, *and* c) **3** *in DMF/toluene 1:1* (*v*/*v*). The * is referenced to DPPH trace (see *Exper. Part*).

symmetric Cu^{II} complex with a tetragonal geometry. Since the spectrum features have $g_{//}$ (*ca.* 2.22) > $g_{\perp}$ (*ca.* 2.05) > g_e (2.0023), the ground-state magnetic orbital containing the unpaired electron corresponds to $d_{x^2-y^2}$ as expected for an axially symmetric complex [23][24] in a square-planar, square-pyramidal, or octahedral geometry with a *Jahn–Teller* effect or a slight equatorial distortion. It appears that a trigonal-bipyramidal geometry can be excluded [25]. The g values and the $A_{//}$ hyperfine coupling constants for the complexes **2** and **3** are very close to those found for Cu^{II} complexes with open chain [26–28] or macrocyclic [29] ligands, and are consistent with a square-pyramidal coordination geometry [26] with slight tetrahedral distortions, as shown in their X-ray structures ($\tau = 0.21$ and 0.18 for **2** and **3**, resp.). The EPR data are, thus, in full agreement with the ligand-field spectra of these complexes (one symmetrical d-d transition band with $\varepsilon \gg 100$ м$^{-1}$ cm^{-1}). These findings, in agreement with the result obtained by the X-ray structure of **2**, show that the structural arrangement is maintained in solution. For complex **3**, a spectrum similar to that of compound **2** is obtained. This is unexpected regarding the trinuclear nature of **3**: the two terminal Cu^{2+} ions are in the same coordination geometry due to the existence of an inversion center, while the third, central Cu^{2+} ion is in a near square planar geometry with two weakly coordinated perchlorate anions (Cu(2)–O(perchlorate) = 2.782(2) Å). Thus, the existence of these two different Cu coordination schemes should give an additional set of lines in the EPR spectrum of **3**, what is not the case. In fact, the well-resolved four parallel lines and the absence of signal at half-field ($g \approx 4$) characteristic of a triplet spin state [30] indicate that the trinuclear complex probably dissociates in solution to give the mononuclear complex **2**. However, the EPR spectra of compounds **2** and **3** recorded in the polycrystalline state are also similar to each other, and similar to those obtained in solution. There is no dipole–dipole interaction between two adjacent Cu^{II} atoms.

Table 3. *EPR Parameters for Complexes* **1**–**3** *in Frozen* (100 K) *and Fluid* (293 K) *DMF/Toluene 1 : 1 Solution*

	$g_{//}$	$g_{\perp}$	$A_{//}$ [10^{-4} cm^{-1}]	$A_{\perp}$ [a] [10^{-4} cm^{-1}]	$g_{//}$ / $A_{//}$ [cm]	g_{iso} (calc. [b])	A_{iso} [10^{-4} cm^{-1}]
1	2.20	2.08	146	38	151	2.12 (2.12)	74
2	2.22	2.05 2.06 [c]	181	19	123	2.11 (2.11)	73
3	2.22	2.05 2.06 [c]	180	21	123	2.11 (2.11)	74
[Cu(dota)]$^{2-}$ [d]	2.30	2.06	150	–	153	–	–
[Cu{Me_2(Me_2NCOCH_2)$_2$-cyclam}]$^{2+}$ [e]	2.24	2.05	156	–	143	–	–
[Cu{(Picolyl)$_2$cyclam}]$^{2+}$ [f]	2.21	–	179	–	123	–	–

[a]) Calculated from $A_{\perp} = (3A_{iso} - A_{//})/2$. [b]) Calculated from $g_{iso} = \left(g_{//} 2g_{\perp}\right)/3$. [c]) Measured in a 3% dispersion of the complex in $MgSO_4$. [d]) [1,4,7,10-Tetraazacyclododecane-1,4,7,10-tetraacetato(4–)]-copper(2–), see [34]. [e]) *trans*-III-Stereoisomer of (*N,N,N′,N′*-4,11-hexamethyl-1,4,8,11-tetraazacyclotetradecane-1,8-diacetamide)copper(2+), see [35]. [f]) *trans*-III-Stereoisomer of (1,8-bis(pyridin-2-ylmethyl)-1,4,8,11-tetraazacyclotetradecane)copper(2+), see [36].

Peculiar behavior is observed for complex **1** since the EPR parameters display a significantly smaller $A_{//}$ coupling constant. According to ligand-field theory [31–33], the $g_{//}$ value increases and the $A_{//}$ value decreases as the equatorial ligand field becomes

weaker [28][31][32] and as the axial one becomes stronger due to a lower overlap between the magnetic orbital $d_{x^2-y^2}$ and the ligand orbitals. This occurs with the simultaneous red-shift of the d-d absorption bands in the electronic spectrum. The $g_{//}/A_{//}$ value can be used as a rough estimate of the coordination geometry, with values of 110–120 cm describing planar-tetragonal complexes, 120–150 cm being typical of slight to moderate distortions, and higher values indicating considerable distortions.

In the case of **1**, the smaller $A_{//}$ and higher $g_{//}/A_{//}$ values compared to **2** and **3** are not indicative of a distortion in the equatorial mean plane but rather of a higher axial-ligand-field strength due to the axial coordination of two N-atoms of the tpaa ligand. The EPR spectrum is thus characteristic of a hexacoordinated complex with a strong axial ligand field, with short axial Cu–N bonds, and a weak equatorial-ligand-field strength. These results are in agreement with other EPR data of hexacoordinated tetraazamacrocyclic Cu^{II} complexes [34][35] (see *Table 3*), which exhibit a distorted octahedral coordination geometry. Hence, the spectroscopic data (UV/VIS and EPR) of complex **1** indicate a hexacoordination of its Cu^{2+} ion.

2.6. *Redox Studies.* To characterize the difference in the coordination environment among Cu^{II} complexes, their redox potentials were determined by cyclic voltammetry in MeCN at room temperature with tetrabutylammonium hexafluorophosphate ($Bu_4N(PF_6)$) as the supporting electrolyte. The half-wave potentials were calibrated with ferrocene as an internal standard and are expressed relative to the normal hydrogen electrode (NHE) [37].

The voltammograms of the three complexes **1**–**3** show cathodic and anodic peaks due to the Cu^{II} reduction and its subsequent oxidation. The suggestion that the redox processes are metal-centered is based on the observation that the free ligand shows no wave in the experimental potential range. The peak-to-peak separation ΔE of each compound is much larger than that of ferrocene, which is known as a reversible couple [37] ($[Cu(tpaa)]^{2+}$, $E_{1/2} = -0.42$ V and $\Delta E = 115$ mV; $[Cu(tpaaH)]^{3+}$, $E_{1/2} = -0.40$ V and $\Delta E = 120$ mV; $[Cu_3(tpaa)_2(ClO_4)_2]^{2+}$, $E_{1/2} = -0.41$ V and $\Delta E = 140$ mV). So, the electron-transfer processes for the studied complexes exhibit quasi-reversible behavior, which indicates that the reduction of Cu^{II} species is probably complicated by structural changes as inferred by AC-simulated mechanism. These structural changes are generally stereochemical rearrangements necessary to meet the coordination requirements of the reduced species, which contains Cu^{I} atoms. As expected, the number of electrons involved in the reduction processes is a function of the number of Cu-atoms. In fact, we found a one-electron reduction for compounds **1** and **2**, and a two-electron reduction only for the trinuclear complex **3**. For this later complex, voltammograms run at lower sweep rate (10 mV s^{-1}) did not reveal the different natures of the three Cu-atoms. We obtained only one cathodic and one anodic peak, and the half-wave potential for compound **3** is not much greater than that of complex **2**, so we conclude that only the two terminal Cu^{II} ions were reduced to Cu^{I}.

3. Conclusions. – The equilibrium constants of the Cu^{II} chelates with tpaa determined by potentiometry show the formation of $[Cu(tpaaH)]^{3+}$ and $[Cu(tpaa)]^{2}$. In addition, the variable-pH *vs.* UV/VIS spectrophotometry allowed us to determine some complex structures in solution.

In the solid state, the two mononuclear complexes **1** and **2** and one trinuclear complex **3** were isolated. The spectroscopic data (IR, UV/VIS, and EPR) revealed that, in the complex $[Cu(tpaa)](PF_6)_2$ (**1**), the Cu^{2+} ion exhibits tetragonal-distorted octahedral geometry. The X-ray crystal structure shows that the protonated mononuclear compound $[Cu(tpaaH)](ClO_4)_3 \cdot H_2O$ (**2**) has distorted square-pyramidal geometry. The proton is bound to one of the three secondary-amine N-atoms, leading to the uncoordination of one arm of the tripodal tpaa ligand. The trinuclear complex $[Cu_3(tpaa)_2(ClO_4)_2](ClO_4)_4 \cdot 2\,H_2O$ (**3**) consists of two mononuclear moieties of **1** bound to the third Cu^{2+} ion by the two free unprotonated (pyridinylmethyl)amino groups. The hexacoordination of the third central Cu^{II} atom is achieved by the ligation of O-atoms of two perchlorate ligands.

Experimental Part

1. *General.* All solvents were purified by conventional procedures [38] and distilled prior to use. All the chemicals commercially available (*Aldrich*) were used as supplied without further purification. The ligand, tris{2-[(2-pyridin-2-ylmethyl)amino]ethyl}amine (= *N′*-(pyridin-2-ylmethyl)-*N*,*N*-bis{2-[(pyridin-2-ylmethyl)amino]ethyl}ethane-1,2-diamine; tpaa) was prepared by the method reported in [6]. Elemental analyses (C, H, and N) were carried out with a *Perkin-Elmer 2400-C,H,N* analyzer in our university. The metal percentage was performed on a *Varian Liberty II ICP-AES* apparatus. Magnetic susceptibilities were determined at room temperature (20°) with $[HgCo(SCN)_4]$ as a calibrant; diamagnetic susceptibility corrections were calculated from *Pascal*'s constants [39].

UV/VIS Spectra: for aq. solns. in quartz cells (1-cm path length), a *Shimadzu UV-2401-PC* spectrophotometer equipped with a standard syringe sipper and a temp.-controlled cell holder *TCC-240 A* was used; for solid complexes, a *Beckman 5240* spectrophotometer (in solid state) was used by depositing the compound on *Schleicher & Schuell* ash-free filter paper, paper without compound was used as reference; for DMF solns., a *Perkin-Elmer Lambda 6* spectrophotometer was used; λ_{max} in nm, ε in $M^{-1}\,cm^{-1}$. IR Spectra: KBr pellets; *Nicolet Avatar-320* spectrometer; $\tilde{\nu}$ in cm^{-1}. EPR Measurements: *Bruker ESP-300* apparatus at the X-band (9.638 GHz), equipped with a double cavity and a liq.-N_2 cooling accessory; recording at 100 kHz modulation frequency and a microwave power of 6 mW, at 293 K and 100 K in DMF/toluene 1:1 (*v*/*v*) (*ca.* 5 mM) or in the solid state with 3% (*w*/*w*) $MgSO_4$ dispersions; referenced to 2,2-diphenyl-1-picrylhydrazyl (DPPH) (g = 2.0036).

2. *Synthesis of Copper(II) Complexes.* ***Caution***! Although we have experienced no problems while handling any of the substances described herein, readers are cautioned to handle them as *potentially explosive compounds.*

*{*N*′-(Pyridin-2-ylmethyl)-*N,N*-bis{2-{[(pyridin-2-yl-*κ*N)methyl]amino-*κ*N}ethyl}ethane-1,2-dianine-*κ*N,*κ*N′}-copper(2+) Bis(hexafluorophosphate)* (*[Cu(tpaa)](PF$_6$)$_2$*; **1**). A mixture of $AcONa \cdot 3\,H_2O$ (0.68 g, 5 mmol) and tpaa · 5 HCl (0.62 g, 1 mmol) in abs. EtOH (30 ml) was stirred an heated to reflux for 10 min on a water bath and then cooled. The precipitated NaCl was filtered off. $Cu(ClO_4)_2 \cdot 6\,H_2O$ (0.36 g, 1 mmol) in abs. EtOH (20 ml) was added dropwise to the filtrate, and the soln. was stirred for 10 min at r.t. A slight excess of solid $NH_4(PF_6)$ (0.41 g, 2.5 mmol) in H_2O (10 ml) was added to the blue soln., and the blue powder that precipitated was filtered off, washed with EtOH and dried *in vacuo*: **1** (*ca.* 50%). M.p. 165°. $\chi_M = 1860 \cdot 10^{-6}$ uem cgs, μ_{eff} = 2.09 BM. UV (MeCN): 680 (70). IR (KBr): 3325*s*, 3291*s* ($\tilde{\nu}$(N–H)); 2940–2850*m*, ($\tilde{\nu}$(C–H)); 1615*s*, 1580*s*, 1479*s*, 1440*s*, 610*s* ($\tilde{\nu}$(py)); 845 v*s* ($\tilde{\nu}(PF_6^-)$). Anal. calc. for $C_{24}H_{33}CuN_7O_8P_2$: C 37.3, H 4.3, Cu 8.2, N 12.7; found: C 37.4, H 4.1, Cu 7.9, N 12.5.

*{*N*-{2-{Bis{2-{[(pyridin-2-yl-*κ*N)methyl]amino-*κ*N}ethyl}amino-*κ*N}ethyl}pyridine-2-methanaminium}-copper(3+) Tris(perchlorate) Hydrate* (*[Cu(tpaaH)](ClO$_4$)$_3$·H$_2$O*; **2**). To a soln. of tpaa · 5 HCl (0.62 g, 1 mmol) in H_2O (30 ml) and $Cu(ClO_4)_2 \cdot 6\,H_2O$ (0.36 g, 1 mmol) was added in small portions solid Na_2CO_3 to adjust the pH at *ca.* 3.5. The mixture was stirred for 10 min (to eliminate CO_2 which evolves), and 0.2M $NaClO_4$ in EtOH (20 ml) was added. The mixture was filtered and set aside at r.t. Blue crystals suitable for X-ray diffraction were isolated after two months: **2** (*ca.* 55%). M.p. 180°. $\chi_M = 1750 \cdot 10^{-6}$ uem cgs, μ_{eff} = 2.04 BM. *UV* (MeCN): 668 (148). IR (KBr): 3325*s*, 3225*s*, ($\tilde{\nu}$(N–H)); 2940–2850*m*, ($\tilde{\nu}$(C–H)); 1610*s*, 1570*s*, 1481*s*, 1445*s*

($\tilde{\nu}$(py)); 1100 v*s* ($\tilde{\nu}$(ClO_4^-)). Anal. calc. for $C_{24}H_{36}Cl_3CuN_7O_{13}$: C 36.0, H 4.5, Cu 7.9, N 12.2; found: C 36.2, H 4.2, N 12.0, Cu 8.1.

*Bis(perchlorato-*κ*O)bis{*μ^3*-[N′-[(pyridin-2-yl-*κ*N)methyl]-*N,N*-bis{2-{[(pyridin-2-yl-*κ*N)methyl]amino-*κ*N}ethyl}ethane-1,2-diamine-*κ*N:*κ*N′}}tricopper(4+) Tetrakis(perchlorate) Dihydrate [*$Cu_3(tpaa)_2(ClO_4)_2$*]-(*ClO_4*)$_4$ 2 *H_2O*; **3**).* A mixture of NaOAc·3 H_2O (0.68 g, 5 mmol) and tpaa·5 HCl (0.62 g, 1 mmol) in abs. EtOH (30 ml) was stirred and heated to reflux for 10 min on a water bath and then cooled. The precipitated NaCl was filtered off. $Cu(ClO_4)_2 \cdot 6\ H_2O$ (0.54 g, 1.5 mmol) in abs. EtOH (20 ml) was added dropwise to the filtrate, and the soln. was stirred for 10 min at r.t. (the formed precipitate was redissolved by adding a few drops of H_2O). The mixture was stirred for further 10 min, and the obtained blue soln. filtered and set aside at r.t. Blue crystals suitable for X-ray diffraction were isolated after 4 weeks: **3** (*ca.* 65%). M.p. 170°. $\chi_M = 1750 \cdot 10^{-6}$ uem cgs per Cu^{2+} ion, $\mu_{eff} = 2.04$ BM per Cu^{2+} ion. UV (MeCN): 615 (323). IR (KBr): 3325*s*, 3225*s* ($\tilde{\nu}$(N−H)); 2940–2850*m*, ($\tilde{\nu}$(C−H)); 1615*s*, 1580*s*, 1475*s*, 1440*s* ($\tilde{\nu}$(py)); 1100 vs, ($\tilde{\nu}$(ClO_4^-)). Anal calc. for $C_{48}H_{70}Cl_6Cu_3N_{14}O_{26}$: C 34.7, H 4.2, Cu 11.5, N 11.8; found: C 34.5, H 4.3, Cu 11.3, N 11.9.

2. *Physical Measurements.* 2.1. *Protometric Measurements.* Stock solns. of $CuSO_4$ (*Fluka*) were standardized with H_4edta (pH 10, 60°, PAN as an indicator). The solns. of strong base (KOH) and strong acid (HNO_3) were prepared from standardized 1M solns. (*Prolabo*). Protometric titrations were performed at 25° under an N_2 stream, with a *Metrohm 665* dosimat. pH Measurements were carried out with a *Metrohm 654* pH-meter equipped with a combined glass electrode (filled with 3M KCl). For the standardization, 0.01M HNO_3 solns. were used. The ionic strength of the solns. was adjusted to 1M with KNO_3 (*Fluka*). The solns. of the ligand alone and in the presence of Cu^{2+} were titrated with 0.1M KOH. The concentrations of tpaa ranged from $1.29 \cdot 10^{-3}$ to $4.29 \cdot 10^{-3}$ M (L/Cu ratios from 1.0 to 9.8). One of the equilibrium constants was determined by fitting the titration curves with the least-squares refinement program PROTAF [11]. Furthermore, for some complexes frequently occurring at high pH values, the determination of the ionic product of H_2O under similar conditions was required. This was performed by refining titration curves of acetic acid, a simple system which does not implicate equilibriums above pH 8. Some measurements required low pH values, so the electrode was calibrated in the range pH 0–2 (where its response is not linear) with increasing amounts of $HClO_4$ ($pH = -\log C_{HClO_4}$).

2.2. *Crystal-Structure Determination*[2]). In *Table 1* are summarized the pertinent crystallographic data together with refinement details for the complexes [Cu(tpaaH)]$(ClO_4)3 \cdot H_2O$ (**2**) and $[Cu_3(tpaa)_2](ClO_4)_6 \cdot 2\ H_2O$ (**3**). Blue block crystals of **2** and **3** were mounted on a glass fiber in a random orientation. Intensity-data collection was carried out with a *Siemens SMART* three-circle diffractometer equipped with a *CCD* bidimensional detector, at a monochromatized wavelength (λ(Mo-K_α) 0.71073 Å), operating at 50 kV and 40 mA. A hemisphere of intensity data was collected at r.t. in 1271 frames (width of 0.30° and exposure time of 10 s per frame).

The structure was solved by the direct methods and refined by full-matrix least squares based on F^2 with the SHELX-TL software package [40]. Empirical absorption correction based on symmetric equivalent reflections was applied with the SADABS program [41]. All H-atom positions were initially located in the difference map, and, for the final refinement, the H-atoms were placed geometrically and held in the riding mode. The last cycles of the refinement included atom positions for all the atoms, anisotropic thermal parameters for all non-H-atoms, and isotropic thermal parameters for all the H-atoms.

2.3 *Electrochemical Measurements.* Cyclic voltammograms were run on an *Autolab PGSTAT12*, connected to a conventional three-electrodes cell system. A 2-mm Pt-disk was used as working electrode, a Pt-wire as counter-electrode, and Ag/Ag^+ as reference electrode. The reference electrode was calibrated to give $E_{1/2} =$ 0.40 V for the ferrocene/ferrocenium couple used as internal reference. The scan rate was 100 $mV \cdot s^{-1}$ for all the three complexes. Ferrocene was found to have a peak separation $\Delta E = |E_{p_a} - E_{p_c}| = 82$ mV at a scan rate of 100 $mV \cdot s^{-1}$ in our system. All the potentials are expressed relative to NHE, by taking into account that $E^0_{Ag/Ag+}$ (MeCN) *vs.* NHE (H_2O) is 0.64 V [42]. MeCN was purified by standard methods, while $Et_4N(ClO_4)$ was recrystallized from H_2O before use. The Cu^{II} complexes ($1.5 \cdot 10^{-3}$ M) was dissolved in deoxygenated MeCN containing 0.1M $Bu_4N(PF_6)$. All solns. were kept under N_2 at r.t. during electrochemical measurements.

---

[2]) CCDC-244990 and CCDC-244991 contain the supplementary crystallographic data for [Cu(tpaaH)] $(ClO_4)_3 \cdot H_2O$ (**2**) and $[Cu_3(tpaa)_2(ClO_4)_2]$ $(ClO_4)_4 \cdot 2\ H_2O$ (**3**), respectively. These data can be obtained free of charge from the *Cambridge Crystallographic Data Centre via* www.ccdc.cam.ac.uk/data_request/cif.

REFERENCES

[1] A. Messerschmidt, in 'Bioinorganic Chemistry of Copper', Eds. K. D. Karlin and Z. Tyeklar, Chapman & Hall, New York, 1993, p. 471; A. Messerschmidt, H. Luecke, R. Huber, *J. Mol. Biol.* **1993**, *230*, 997; A. Messerschmidt, W. Steigemann, R. Huber, G. Lang, P. M. H. Kroneck, *Eur. J. Biochem.* **1992**, *209*, 597; A. Messerschmidt, R. Ladenstein, R. Huber, M. Bodognesi, L. Avigliano, R. Petruzzelli, A. Rossi, A. Finazzi-Agro, *J. Mol. Biol.* **1992**, *224*, 179.

[2] I. Zaitseva, V. Zaitsev, G. Karl, K. Moshkov, B. Bax, A. Ralph, P. Lindley, *J. Biol. Chem.* **1996**, *1*, 15.

[3] P. Gamez, P. G. Aubel W. L. Driessen, J. Reedijk, *Chem. Soc. Rev.* **2001**, *30*, 376; A. L. Gavrilova, B. Bosnich, *Chem. Rev.* **2004**, *104*, 349, and refs. cit. therein; 'Biomimetic Oxidation Catalysed by Transition Metal Complexes', Ed. B. Meunier, Imperial College Press, London, 2000, and refs. cit. therein.

[4] A. Mohamadou, C. Jubert, N. Gruber, J. P. Barbier, *Eur. J. Inorg. Chem.* **2004**, 1285.

[5] C. Jubert, A. Mohamadou, J. Marrot, J. P. Barbier, *J. Chem. Soc., Dalton Trans.* **2001**, 1230.

[6] A. Mohamadou, C. Gérard, *J. Chem. Soc., Dalton Trans.* **2001**, 3320.

[7] T. Nagano, T. Hirano, M. Hirobe, *J. Biol. Chem.* **1989**, *264*, 9243; T. Nagano, T. Hirano, M. Hirobe, *Free Radical Res. Commun.* **1991**, *12–13*, 221; R. H. Weiss, A. G. Flickinger, W. J. Rivers, M. H. Hardy, K. W. Aston, U. S. Ryan, D. P. Riley, *J. Biol. Chem.* **1993**, *268*, 23049.

[8] I. Morgenstern-Badarau, F. Lambert, J. P. Renault, M. Cesario, J. D. Marechal, F. Maseras, *Inorg. Chim. Acta* **2000**, *297*, 338.

[9] A. Deroche, I. Morgenstern-Badarau, M. Cesario, J. Gulhem, B. Keita, L. Nadjo, C. Houée-Levin, *J. Am. Chem. Soc.* **1996**, *118*, 4567.

[10] J. R. Hartman, R. W. Vachet, J. H. Callhan, *Inorg. Chim. Acta* **2000**, *297*, 79.

[11] R. Fournaise, C. Petitfaux, *Talanta* **1987**, *34*, 385; R. Fournaise, C. Petitfaux, *Analusis* **1990**, *18*, 242.

[12] L. Alderigui, P. Gans, A. Ienco, D. Peters, A. Sabatini, A. Vacca, *Coord. Chem. Rev.* **1999**, *184*, 311.

[13] E. G. Bakalbassis, J. Mrozinski, C. A. Tsipis, *Inorg. Chem.* **1985**, *24*, 3548; R. Barbucci, G. Cialdi, G. Ponticelli, P. Paoletti, *J. Chem. Soc., A* **1969**, 1775; B. J. Hathaway, I. M. Procter, R. C. Slade, A. A. G. Tomlinson, *J. Chem. Soc., A* **1969**, 2219; R. C. Slade, A. A. G. Tomlinson, B. J. Hathaway, D. E. Billing, *J. Chem. Soc., A* **1968**, 61.

[14] J. Gazo, I. B. Bersuker, J. Garaj, M. Kabesova, J. Kohout, H. Langfelderova, M. Melnyk, M. Serator, F. Valach, *Coord. Chem. Rev.* **1976**, *19*, 253.

[15] C. Jubert, A. Mohamadou, E. Guillon, J. P. Barbier, *Polyhedron* **2000**, *19*, 1447.

[16] M. Ray, R. Mukherjee, J. F. Richardson, M. S. Mashuta, R. M. Buchanan, *J. Chem. Soc., Dalton Trans.* **1999**, 1131; D. Marcos, R. Martinez-Manez, J. V. Folgado, A. Bertran-Porter, D. Bertran-Porter, A. Fuertes, *Inorg. Chim. Acta* **1989**, *159*, 11.

[17] E. Billo, *Inorg. Nucl. Chem. Lett.* **1974**, *10*, 613.

[18] A. W. Addison, T. N. Rao, J. Reedijk, J. Van Rijn, G. C. Verschoor, *J. Chem. Soc., Dalton Trans.* **1984**, 1349.

[19] J. R. Hartman, R. W. Vachet, W. H. Pearson, R. J. Wheat, J. H. Callahan, *Inorg. Chim. Acta* **2003**, *343*, 119.

[20] J. R. Hartman, A. L. Kammier, R. J. Spracklin, W. H. Pearson, M. Y. Combariza, R. W. Vachet, *Inorg. Chim. Acta* **2004**, *357*, 1141.

[21] M. Ray, S. Mukherjee, R. N. Mukherjee, *J. Chem. Soc., Dalton Trans.* **1990**, 3635; M. Ray, R. N. Mukherjee, *Polyhedron* **1992**, *11*, 2929.

[22] B. J. Hathaway, I. M. Procter, R. C. Slade, A. A. G. Tomlinson, *J. Chem. Soc., A* **1968**, 1678;

[23] B. J. Hathaway, in 'Comprehensive Coordination Chemistry', Eds. G. Wilkinson, R. D. Gillard, and J. A. McCleverty, Pergamon, Oxford, 1987, Vol. 5, p. 533–594 and 662.

[24] J. R. Pilbrow, 'Transition Ion Electron Paramagnetic Resonance', 1st edn., Clarendon Press, Oxford, 1990.

[25] B. J. Hathaway, *Coord. Chem. Rev.* **1983**, *52*, 87.

[26] G. A. McLachlan, G. D. Fallon, R. L. Martin, L. Spiccia, *Inorg. Chem.* **1995**, *34*, 254.

[27] J. A. Halfen, J. M. Uhan, D. C. Fox, M. P. Mehn, L. Que Jr., *Inorg. Chem.* **2000**, *39*, 4913.

[28] E. V. Rybak-Akimova, A. Y. Nazarenko, L. Chen, P. W. Krieger, A. M. Herrera, V. V. Tarasov, P. D. Robinson, *Inorg. Chim. Acta* **2001**, *324*, 1.

[29] S. J. Brudenell, L. Spiccia, E. R. T. Tiekink, *Inorg. Chem.* **1996**, *35*, 1974; L. Siegfried, C. N. McMahon, T. A. Kaden, C. Palivan, G. Gescheidt, *Dalton Trans.* **2004**, 2115.

[30] S. Brandès, C. Gros, F. Denat, P. Pullumbi, R. Guilard, *Bull. Soc. Chim. Fr.* **1996**, *133*, 65; M. Lachkar, R. Guilard, A. Atmani, A. DeCian, J. Fischer, R. Weiss, *Inorg. Chem.* **1998**, *37*, 1575; J. M. Rowland, M. M. Olmstead, P. K. Mascharak, *Inorg. Chem.* **2000**, *39*, 5326; S. Carvalho, C. Cruz, R. Delgado, M. G. B. Drew, V. Félix, *J. Chem. Soc., Dalton Trans.* **2003**, 4261.

[31] U. Sakaguchi, A. W. Addison, *J. Chem. Soc., Dalton Trans.* **1979**, 600.
[32] K. Miyoshi, H. Tanaka, E. Kimura, S. Tsuboyama, S. Murata, H. Shimizu, K. Ishizu, *Inorg. Chim. Acta* **1983**, *78*, 23.
[33] M. J. Maroney, N. J. Rose, *Inorg. Chem.* **1984**, *23*, 2252.
[34] J. Costa, R. Delgado, M. D. C. Figueira, R. T. Henriques, M. Teixeira, *J. Chem. Soc., Dalton Trans.* **1997**, 65.
[35] C. Bucher, E. Duval, J.-M. Barbe, J.-N. Verpeaux, C. Amatore, R. Guilard, *C. R. Acad. Sci. Paris, Série IIc* **2000**, *3*, 211.
[36] A. E. Goeta, J. A. K. Howard, D. Maffeo, H. Puschmann, J. A. G. Williams, D. S. Yufit, *J. Chem. Soc., Dalton Trans.* **2000**, 1873.
[37] R. R. Gagne, C. A. Koval, G. C. Lisensky, *Inorg. Chem.* **1980**, *19*, 2855.
[38] D. Perrin, W. L. F. Armarego, R. D. Perrin, 'Purification of Laboratory Chemicals', 3rd edn., Pergamon, Oxford, 1988.
[39] A. Earnshaw, 'Introduction to Magnetochemistry', Academic Press, London, 1968, p. 5.
[40] G. M. Sheldrick, 'SHELXTL NT, v. 5.10', 1999, Bruker AXS, Inc., Madison, Wisconsin 53719, USA.
[41] G. M. Sheldrick, 'SADABS, Program for Scaling and Correction of Area Detector Data', University of Göttingen, Germany, 1997; R. Blessing, *Acta Crystallogr.*, *Sect. A* **1995**, *51*, 33.
[42] S. I. Chan, H. H. T. Nguyen, A. K. Shiemke, M. E. Lindstrom, in 'Bioinorganic Chemistry of Copper', Eds. K. D. Karlin, and Z. Tyeklar, Chapman & Hall, New York, 1993, p. 184.

Received February 22, 2005